Check for updates

Stroke: Vascular and Interventional Neurology

ORIGINAL RESEARCH

A Novel Application of Radiomics Analysis for the Evaluation of Centroid Radii Model Texture on the Surface of Cerebral Aneurysms

Alexandra Lauric, PhD; Adel M. Malek, MD, PhD

BACKGROUND: The centroid radii model (CRM)—defined as the distance from aneurysm surface points to the centroid—has shown promise in distinguishing ruptured from unruptured intracranial aneurysms by capturing morphological characteristics. We propose a novel application of radiomics for analyzing CRM texture and patterns, extending radiomics beyond medical imaging-based analysis.

METHODS: Three-dimensional rotational angiographic volumes from 187 aneurysms (49 ruptured) were analyzed. Aneurysm surfaces were segmented and converted to uniform triangular meshes. Established size and shape metrics (size, height, aspect ratio, height/width, size ratio, and nonsphericity) and CRM values were computed. CRM data were projected onto a unit sphere and mapped to grayscale images for radiomics analysis. Univariate and multivariate analyses were used to evaluate the established features and 93 radiomics features for the accuracy of rupture status discrimination.

RESULTS: Ruptured aneurysms exhibited greater CRM texture complexity and heterogeneity, with higher entropy, variance, contrast, and gray-level nonuniformity. These aneurysms had localized high CRM intensities and widespread low CRM regions, as well as reduced pattern uniformity. All established morphological features were significantly elevated in ruptured aneurysms. Multivariate regression using radiomics features resulted in an area under the curve of 0.86 (specificity 0.81, sensitivity 0.78), compared with conventional features (area under the curve 0.82, specificity 0.75, sensitivity 0.81).

CONCLUSION: Radiomics-based histogram and texture analysis of surface CRM offers strong rupture status discrimination power, which compares favorably with established size and shape features. This novel use of radiomics on surface-based features provides additional insight into the characteristics of ruptured aneurysms and may have potential utility in risk stratification.

Key Words: 3D surface texture ■ centroid radii model ■ intracranial aneurysms ■ ruptured status

Downloaded from http://ahajournals.org by on April 6, 2026

Cerebral aneurysms present in various shapes and sizes, and their morphological features are intensely researched regarding association with the risk of rupture.[1] Although 2-dimensional (2D) aneurysmal features such as size, height/width, and aspect ratio continue to be some of the most

Correspondence to: Adel M. Malek, M.D., Ph.D., Cerebrovascular Hemodynamics Laboratory, Department of Neurosurgery, Tufts Medical Center and Tufts University School of Medicine, 800 Washington Street, Boston, MA 02111, Fax: +1-617-636-7587. E-mail: amalek@tuftsmedicalcenter.org

Supplementary Material for this article is available at https://www.ahajournals.org/doi/suppl/10.1161/SVIN.125.001909

IRB approval: This research was approved by Tufts Health Sciences Campus Institutional Review Board (IRB# 9035). Patient consent was waived because of the retrospective nature of the study not affecting patient clinical care.

This manuscript was sent to Dr. Andrei V. Alexandrov, Guest Editor, for review by expert referees, editorial decision, and final disposition.

© 2025 The Author(s). Published on behalf of the American Heart Association, Inc., and the Society of Vascular and Interventional Neurology by Wiley Periodicals LLC. This is an open access article under the terms of the Creative Commons Attribution-NonCommercial License, which permits use, distribution and reproduction in any medium, provided the original work is properly cited and is not used for commercial purposes.

Stroke: Vascular and Interventional Neurology is available at: www.ahajournals.org/journal/svin

relevant clinical features, many additional parameters have been introduced to quantify aneurysmal morphology. Three-dimensional (3D) morphological parameters such as nonsphericity, ellipticity, and undulation indices were among the first features proposed to describe aneurysmal shapes.[2,3] More complex shape analysis, however, has been investigated using geometric and Zernike moments,[4] Fourier analysis,[5] surface curvature analysis,[2] writhe number distribution analysis,[6] and centroid radii model (CRM).[7] Previously, distribution moments of CRM, a scalar field computed by measuring Euclidean distance from surface points to the geometric centroid of the aneurysmal sac, were evaluated for rupture status classification.[7]

Recently, PyRadiomics,[8] an automatic image processing tool that quantifies textural information from medical images, has been employed for intracranial aneurysms morphological evaluation.[9–13] Use of radiomics, which allows for the evaluation of both shape morphology and intensity-based descriptors (histogram, texture, and patterns), assumes that biomedical images contain disease-specific information that is not perceptible through visual inspection and traditional processing tools.

For cerebral aneurysm evaluation, the use of radiomics has mostly been restricted to morphological analysis[9–13] because of intensity homogeneity due to contrast-enhanced catheter rotational angiography imaging, which renders texture evaluation less relevant for these volumes. Emerging research is exploring the use of radiomics texture and pattern analysis on angiographic aneurysmal data.[14–16]

We propose a method to extend the use of radiomics to surface-based scalar fields derived from aneurysm morphology, extending its use beyond the evaluation of medical imaging data. Specifically, we introduce an in-depth evaluation of not only the distribution but also the texture and patterns of the CRM on the surface of intracranial aneurysms–a new application of radiomics that is not directly related to medical imaging analysis. Demonstrated on CRM parameters, this approach can be extended to any surface-based feature describing local morphology.

Nonstandard Abbreviations and Acronyms

CRM centroid radii model

CLINICAL PERSPECTIVE

What Is New?

- We introduce a novel radiomics-based method to analyze surface scalar maps derived from aneurysm morphology, demonstrated on centroid radii model data, enabling detailed evaluation of shape textures and patterns beyond traditional volumetric imaging.

What Are the Clinical Implications?

- Radiomics analysis of centroid radii model - derived surface textures and patterns enables accurate discrimination of aneurysm rupture risk, supporting improved identification of high-risk aneurysms for closer monitoring or early intervention.
- This approach adds to our understanding of the role of aneurysm surface morphology in the mechanism of rupture and provides new insights into the characteristics of ruptured aneurysms.
- The method can be extended beyond centroid radii model to other surface scalar maps, such as curvature or other surface metrics, offering a flexible and powerful tool for comprehensive risk assessment.

METHODS

Data are available upon reasonable request. Study data are from our clinical imaging repository, and as such contain patient identification, and cannot be shared in its raw state. De–identified models may be available upon reasonable request made to the corresponding author.

Patient Selection

High-resolution 3-D catheter angiographic volumetric data sets were available for 187 intracranial aneurysms (49 ruptured). All imaging of the ruptured subset was obtained within 48 hours of rupture to avoid vasospasm onset. This research was approved by the institutional review board ethics committee. Patient consent was waived because of the retrospective nature of the study not impacting patient clinical care.

Angiography and Data Processing

Three-dimensional catheter-based cerebral angiograms were obtained using a Siemens Artis (Malvern, PA) calibrated biplane system. Volumetric angiographic data were reconstructed into 3D data sets using standard clinical software. Aneurysm and

Downloaded from http://ahajournals.org by on April 6, 2026

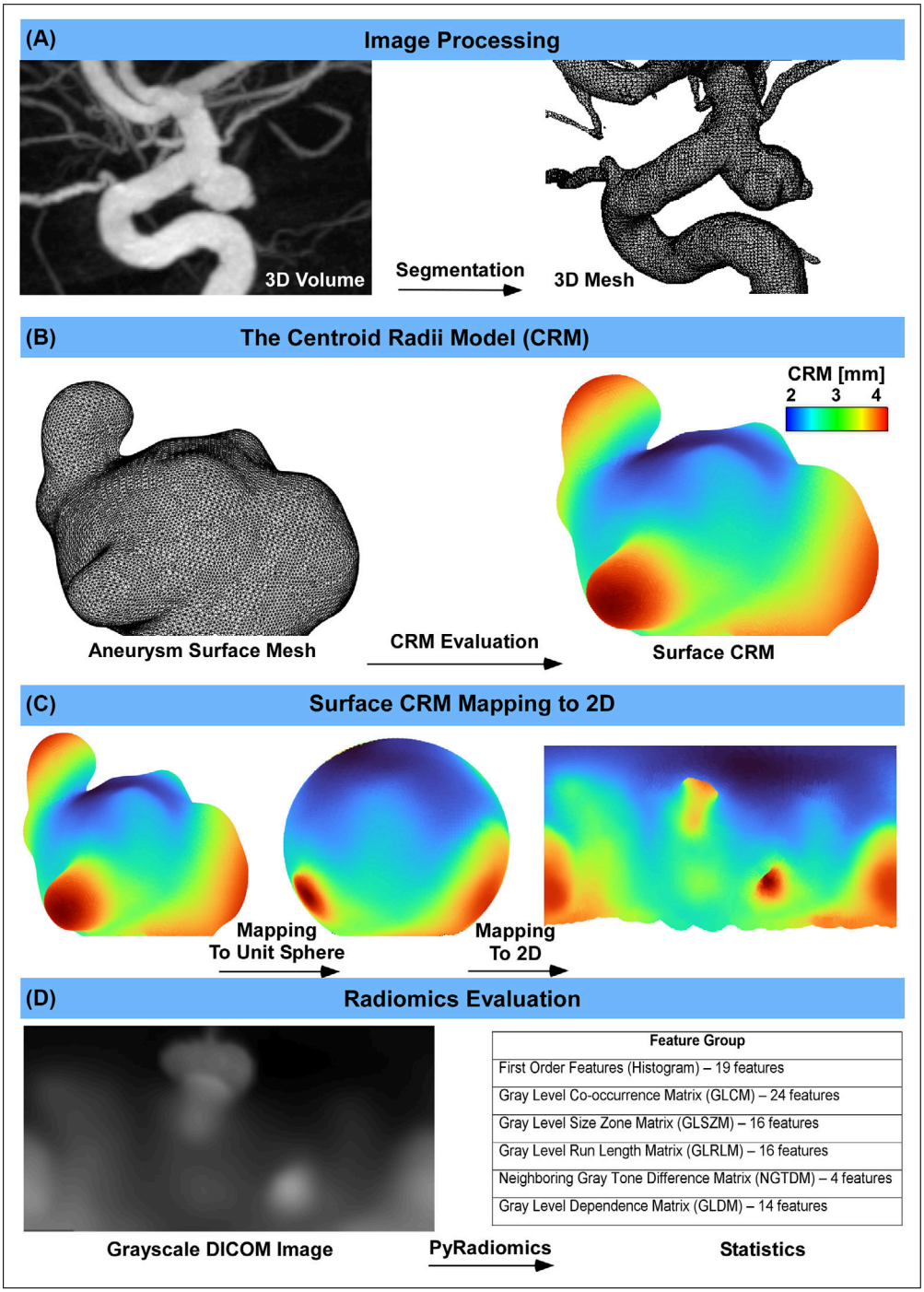


Figure 1. Processing steps of the CRM radiomics analysis. A, 3D aneurysmal models are segmented from angiographic data. **B,** CRM is computed as the distance from each mesh vertex to the aneurysm centroid. **C,** Surface CRM is projected to the unit sphere and mapped to 2D images. **D,** Corresponding grayscale images are the input to radiomics. Radiomics features are generated and evaluated as rupture status discriminants using univariate and multivariate statistical analysis. 2D indicates 2-dimensional; 3D, 3-dimensional; CRM, centroid radii model; and DICOM, Digital Imaging and Communications in Medicine.

vessel surfaces were manually segmented in 3D using Amira software (version 5.3.3, Thermo Fisher Scientific, Waltham, MA) (Figure 1A). Segmented volumes were exported as uniform-resolution triangular meshes representing the aneurysm surface (Figure 1B).

From each surface mesh, basic morphological features including maximum diameter, maximum height, height-to-width ratio, aspect ratio, size ratio, and nonsphericity index were computed as described in the literature.[12,17]

Downloaded from http://ahajournals.org by on April 6, 2026

Centroid-Radii Model Processing

Lauric et al[7] introduced the use of the CRM for describing intracranial aneurysm morphology. CRM was computed for each aneurysm surface by measuring the Euclidean distance from every mesh vertex to the geometric centroid of the aneurysm sac. The resulting CRM distribution formed a scalar field over the aneurysm surface, capturing shape deviation and surface protrusion geometry (Figure 1C).

Mapping 3D Surface CRM to Grayscale Image

To enable radiomics evaluation, the 3D CRM data were mapped to 2D grayscale images using a spherical projection followed by UV mapping.[18] First, each aneurysm surface was translated such that its centroid was placed at the origin. Each vertex was projected onto the unit sphere, and the corresponding CRM value was recorded. To generate a 2D image of CRM distribution, the unit sphere was flattened to 2D using a UV unwrapping algorithm (Figure 1C). CRM values were converted to 8-bit grayscale intensities following scaling by 100, forming the input to the PyRadiomics algorithm (Figure 1D).

Radiomics and Feature Extraction

CRM grayscale images were analyzed using PyRadiomics,[8] a Python-based platform for high-throughput radiomics extraction. A total of 93 radiomics features were extracted for each aneurysm image, spanning the following groups: first-order statistics, gray-level co-occurrence matrix, gray-level size zone matrix, gray-level run length matrix, neighboring gray tone difference matrix, and gray-level dependence matrix. Feature definitions and calculation parameters followed PyRadiomics default settings. These features describe statistical properties of CRM distribution as well as the spatial relationships and patterns of CRM-derived intensities, including frequency of occurrence, size, and distribution of connected components based on specific gray-level values, heterogeneity, and spatial arrangement of regions with distinct intensity patterns, local variation in intensity and contrast, etc. The complete list of radiomics features evaluated in this study is available as supplemental material (Table S1).

Statistical Analysis

Statistical analysis was performed using JMP Pro 17 (SAS Institute, Cary, NC). Univariate analysis was conducted using Student's *t*-test, assuming $P<0.05$ for statistical significance. Receiver operating characteristic curves were generated for each feature, and the area under the curve (AUC) was recorded to evaluate classification performance. Features with AUC>0.75 were considered strong rupture status discriminators.

Multivariate logistic regression was performed using elastic net regularization applied to the radiomics features to reduce overfitting and account for potential correlations among predictors. Analysis was performed separately for size and shape features and radiomics features. Feature selection was integrated within the elastic net framework using 4-fold cross-validation to ensure model robustness and generalizability, with only nonzero coefficient terms retained in the final model as selected predictive features. A maximum of 6 features was included in each model to maintain a 10:1 and 5:1 ratio of samples and positive cases to predictors.[19]

RESULTS

Patient Demographics

A total of 187 aneurysms (49 ruptured, 158 female patients) were included in the final analysis. There was no statistically significant age difference between patients with ruptured and unruptured aneurysms (mean age 60.59±14.79 years versus 55.89±14.31 years, $P = 0.051$).

Size and Shape Feature Analysis

Univariate statistical analysis of established size and shape descriptors revealed significantly higher values for ruptured aneurysms across all parameters. Maximum diameter, maximum height, height/width ratio, aspect ratio, size ratio, and the nonsphericity index were significantly elevated in the ruptured group ($P<0.001$ for all). AUC values ranged from 0.74 to 0.79, with the highest discrimination achieved by aspect ratio and size ratio (AUC = 0.79) (Table 1).

Radiomics Analysis

A complete list of univariate analyses for all radiomics features generated in this study is available as supplemental material (Table S1). Univariate statistical analysis for the selected best-performing features within each radiomics group is available in Table 2.

First-Order Features

This group of features quantifies statistical properties of CRM intensity distribution on the surface. Ruptured aneurysms had significantly higher entropy, intensity range, and variance, whereas unruptured aneurysms had significantly higher uniformity, highlighting the heterogeneous nature of ruptured surfaces.

Downloaded from http://ahajournals.org by on April 6, 2026

Table 1. Univariate Statistical Analysis of Size and Shape Descriptors for Rupture Status Discrimination

Size and shape descriptors	Ruptured	Unruptured	*P* value	AUC
Maximum diameter [mm]	9.8894 ± 4.3934	6.6431 ± 3.335	<0.001	0.75
Maximum height [mm]	8.1952 ± 3.7509	5.0295 ± 2.8731	<0.001	0.78
Height/width	1.2005 ± 0.34308	0.94124 ± 0.22296	<0.001	0.74
Aspect ratio	1.9647 ± 0.98967	1.2715 ± 0.5574	<0.001	0.79
Size ratio	3.21 ± 1.6045	2.0193 ± 1.2145	<0.001	0.79
Nonsphericity index	0.23751 ± 0.073438	0.16068 ± 0.075936	<0.001	0.78

Shown are the mean±SD. Statistical significance was assumed for $P<0.05$. AUC indicates area under the receiver operating characteristic curve.

Table 2. Univariate Statistical Analysis of Selected CRM Radiomics Descriptors for Rupture Status Discrimination

Radiomics descriptors	Ruptured	Unruptured	*P* value	AUC
First-order features				
Entropy	3.491 ± 0.64781	2.7879 ± 0.72013	<0.0001	0.77
Range	314.55 ± 158.03	197.55 ± 108.65	<0.0001	0.76
Uniformity	0.11302 ± 0.048352	0.1918 ± 0.093054	<0.0001	0.77
Variance	6449.4 ± 9511.6	2509.4 ± 3556.3	0.0001	0.76
Gray-level co-occurrence matrix				
ClusterProminence	29060 ± 94154	4590.2 ± 16096	0.0036	0.76
ClusterTendency	63.798 ± 93.49	25.011 ± 35.369	0.0001	0.76
Contrast	0.36723 ± 0.36682	0.18205 ± 0.14018	<0.0001	0.79
DifferenceEntropy	0.8666 ± 0.27497	0.6188 ± 0.22333	<0.0001	0.79
JointAverage	7.0302 ± 3.1677	4.6596 ± 2.4539	<0.0001	0.76
JointEnergy	0.077785 ± 0.045216	0.15672 ± 0.093072	<0.0001	0.77
JointEntropy	4.5457 ± 0.97904	3.5193 ± 1.0149	<0.0001	0.78
MaximumProbability	0.14863 ± 0.068427	0.26209 ± 0.12615	<0.0001	0.78
SumAverage	14.06 ± 6.3355	9.3191 ± 4.9079	<0.0001	0.76
Gray-level size zone matrix features				
ZonePercentage	0.01878 ± 0.028956	0.006536 ± 0.01048	<0.0001	0.80
ZoneVariance	62263 ± 79784	259280 ± 290550	<0.0001	0.79
LowGrayLevelZoneEmphasis	0.066523 ± 0.057025	0.14677 ± 0.093903	<0.0001	0.79
HighGrayLevelZoneEmphasis	110.53 ± 104.5	50.193 ± 48.97	<0.0001	0.77
SmallAreaHighGrayLevelEmphasis	5.716 ± 12.871	1.3888 ± 3.2	0.0003	0.78
LargeAreaLowGrayLevelEmphasis	8.5122 ± 14.605	50.866 ± 79.226	0.0003	0.77
Gray-level run length matrix features				
RunPercentage	0.26825 ± 0.09903	0.17914 ± 0.085424	<0.0001	0.78
RunVariance	27.034 ± 21.157	74.695 ± 68.06	<0.0001	0.78
ShortRunHighGrayLevelEmphasis	43.552 ± 70.192	13.985 ± 26.511	<0.0001	0.77
LongRunLowGrayLevelEmphasis	8.5122 ± 14.605	50.866 ± 79.226	0.0003	0.77
Neighboring gray tone difference matrix features				
Busyness	2.4644 ± 2.4113	5.7418 ± 6.3756	0.0006	0.73
Complexity	31.137 ± 40.836	10.698 ± 17.176	<0.0001	0.77
Contrast 2	0.017037 ± 0.007299	0.012311 ± 0.006627	<0.0001	0.71
Strength	1.5491 ± 2.3413	0.5933 ± 0.95497	0.0001	0.73
Gray-level dependence matrix features				
DependenceVariance	3.5002 ± 0.84251	2.6081 ± 0.81091	<0.0001	0.79
HighGrayLevelEmphasis	76.144 ± 81.051	34.231 ± 42.245	<0.0001	0.76
LargeDependenceHighGrayLevelEmphasis	2874.7 ± 1983.6	1607.5 ± 1495.4	<0.0001	0.75
SmallDependenceHighGrayLevelEmphasis	5.716 ± 12.871	1.3888 ± 3.2	0.0003	0.78

Shown are the mean±SD. Statistical significance was assumed for $P<0.05$. AUC indicates area under the receiver operating characteristic curve.

Downloaded from http://ahajournals.org by on April 6, 2026

Gray-Level Co-Occurrence Matrix Features

This group of features quantifies patterns based on the frequency of specific patterns within the image. Compared with unruptured aneurysms, ruptured aneurysms are characterized by increased complexity and heterogeneity of CRM-derived intensity patterns. They have higher contrast, as well as higher cluster prominence and tendency. In addition, they have increased difference entropy (heterogeneity in magnitude and patterns), increased joint average (distinct areas of high CRM-derived intensities), and increased joint entropy (variability and diversity of intensity patterns) but lower joint energy (a measure of texture homogeneity/uniformity). Moreover, ruptured aneurysms have significantly higher sum average, indicating clusters with contrasting intensity values, again indicating a more heterogeneous and intricate texture pattern. Figure 2 shows examples of ruptured and unruptured aneurysms with clear differences in their CRM texture and patterns.

Gray-Level Size Zone Matrix Features

This group of features quantifies the size distribution of connected regions with specific CRM-derived image intensity. Compared with unruptured aneurysms, ruptured aneurysms are characterized by a high zone percentage (high distribution of smaller connected regions), but low zone variance (less variation in the size of distinct intensity clusters). In addition, ruptured aneurysms have a pronounced prevalence of smaller clusters with high CRM values (larger HighGrayLevelZoneEmphasis and SmallAreaHighGrayLevelEmphasis) compared with unruptured aneurysms, which were characterized by large clusters of low CRM values (higher LowGrayLevelZoneEmphasis and LargeAreaLowGrayLevelEmphasis. Together, the findings suggest that ruptured aneurysms showcase localized concentration of high CRM intensity representative of spatial irregularities, compared with unruptured aneurysms that show intensity homogeneity at low values.

Gray-Level Run Length Matrix Features

This group of features quantifies the distribution of intensity runs (consecutive voxels of the same intensity), providing information regarding texture coarseness. Compared with unruptured aneurysms, ruptured aneurysms are characterized by high nonuniformity features. They have a high run percentage (percentage of consecutive voxels) but a low Run Variance (reduced variability in the length of runs). In addition, ruptured aneurysms have higher ShortRunHighGrayLevelEmphasis with low LongRunLowGrayLevelEmphasis (small regions of intensity spikes). Together, these findings suggest that ruptured aneurysms are characterized by the presence of short and long runs of high CRM values, which are clustered together (low Run Variance).

Neighboring Gray Tone Difference Matrix Features

This group of features quantifies intensity differences between neighboring voxels in the image. Ruptured aneurysms had higher complexity, strength, and contrast but lower busyness, suggesting sharper local changes in CRM values and prominent intensity transitions between neighboring voxels.

Gray-Level Dependence Matrix Features

Features in this group quantify CRM intensity dependencies within a particular size neighborhood. Ruptured aneurysms exhibit significantly higher DependenceVariance, indicating heterogeneity among dependencies in the image, reflecting the presence of distinct regions with different voxel dependencies. HighGrayLevelEmphasis, SmallDependenceHighGrayLevelEmphasis, and LargeDependenceHighGrayLevelEmphasis were significantly higher in the ruptured group compared with the unruptured group, indicating heterogeneity in CRM intensity with small and large-scale geometric variations.

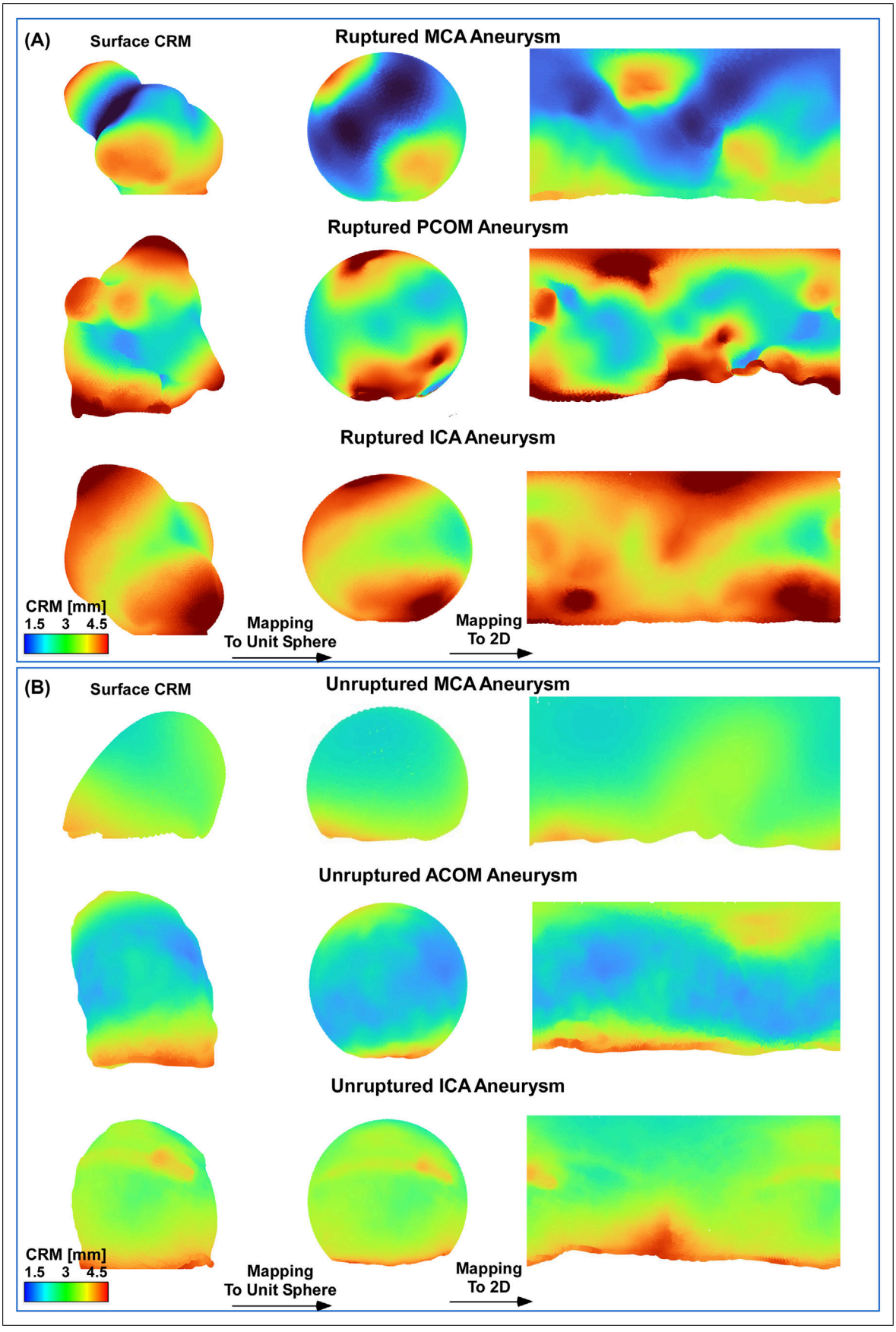
Multivariate Analysis

Elastic net regression with 4-fold cross-validation identified 5 CRM radiomics features as independent predictors of rupture status: Coarseness, LargeAreaHighGrayLevelEmphasis, MaximumProbability, SmallAreaHighGrayLevelEmphasis, and ZoneEntropy.

Among these, Coarseness (estimate: −15.14), LargeAreaHighGrayLevelEmphasis (estimate: −7.91), and MaximumProbability (estimate: −11.09) had negative coefficients, indicating that lower values of these features are associated with increased rupture risk. Specifically, lower coarseness suggests a finer and more irregular surface texture in ruptured aneurysms; lower LargeAreaHighGrayLevelEmphasis reflects a lack of large homogeneous surface regions and instead suggests more fragmented protrusions; and lower MaximumProbability indicates greater heterogeneity in surface CRM intensity.

In contrast, SmallAreaHighGrayLevelEmphasis (estimate: +11.72) and ZoneEntropy (estimate: +1.63) had positive coefficients, meaning higher values are linked to rupture. These findings suggest that ruptured aneurysms are characterized by many small, localized high-intensity surface regions (reflecting localized protrusions or blebs) and higher entropy, consistent

Downloaded from http://ahajournals.org by on April 6, 2026



Downloaded from http://ahajournals.org by on April 6, 2026

Table 3. Multivariate Analysis of Morphological and CRM Radiomics Descriptors for Rupture Status Discrimination

Size and shape descriptors	*P* value	AUC	Specificity/ sensitivity
Nonsphericity index	0.13	0.82	
Size ratio	0.82		Sensitivity 0.81
Height	0.14		Specificity 0.75
Height/width	0.03		
CRM descriptors	***P* value**	**AUC**	**Specificity/ sensitivity**
Coarseness	<0.0001	0.86	
LargeAreaHighGray-LevelEmphasis	0.09		
Maximum Probability	0.06		Sensitivity 0.78
SmallAreaHighGray-LevelEmphasis	0.01		Specificity 0.81
ZoneEntropy	0.37		

Feature selection was performed using an elastic net, using only features with nonzero coefficient terms and retaining up to 6 top features. Shown are *P* value, AUC, and the corresponding sensitivity and specificity values. AUC indicates area under the receiver operating characteristic curve; and CRM, centroid radii model.

with more complex and heterogeneous surface morphology.

The combined multivariate model achieved an AUC of 0.86, with specificity of 0.81 and sensitivity of 0.78 (Table 3). In comparison, the multivariate shape-only model achieved an AUC of 0.82, with a specificity of 0.75 and sensitivity of 0.81.

DISCUSSION

Radiomics, a comprehensive approach for evaluating various aspects of medical imaging data, provides automatic and reproducible assessment of morphological and texture characteristics. In the context of aneurysm evaluation, morphological 2D and 3D radiomics features have previously been proposed as discriminators of rupture status,[9–13] and their comparative value compared with established shape descriptors has been discussed.[10] On the other hand, the use of texture and pattern radiomics features for aneurysmal imaging is a relatively new area of research that is currently emerging in the literature, and radiomics descriptors have been used for pattern analysis on magnetic resonance angiographic aneurysmal data,[14] to analyze angiographic parametric imaging and serve as biomarkers for assessing blood flow contrast within the aneurysmal sac,[15] and to predict the occlusion of aneurysms before and after intervention, offering valuable insights into the treatment outcomes.[16]

Morphological evaluation of aneurysmal shapes is used to assess rupture risk and to inform clinical management. Multiple 2D and 3D features have been introduced and studied, including complex shape analysis such as CRM analysis.[7] CRM represents the distance from each point on the aneurysm surface to the geometric center of the aneurysm, capturing localized protrusions and deviations from spherical geometry. The model captures salient features of the shape, while discarding small shape variations.

In this study, we propose a surface-based application of radiomics texture analysis by evaluating the CRM distributions and patterns mapped from aneurysmal surface meshes. By converting CRM values to grayscale images and applying radiomics extraction, we demonstrate that rupture status is associated with distinct texture signatures.

Radiomics features derived from CRM intensities reveal consistent patterns of increased heterogeneity and localized intensity spikes in the ruptured group. First-order features such as entropy, range, and variance were significantly higher in ruptured aneurysms, indicating a broader spread and complexity in CRM intensity values. Ruptured aneurysms have higher contrast, joint entropy, and difference entropy, further reflecting the irregular and varied spatial distribution of surface shape. Whereas ruptured aneurysms exhibit a high density of small high-intensity zones indicative of surface irregularities and bumps, unruptured aneurysms were associated with larger homogeneous zones of low CRM values, suggesting more sphere-like surfaces. This is further supported by the fact that ruptured aneurysms tend to have numerous short runs of high CRM values and fewer long runs of low values, suggestive of localized protrusions rather than extended flat surfaces. This suggests that ruptured aneurysms not only deviate more from sphericity but also do so in spatially localized regions. Multivariate analysis incorporating 5 CRM radiomics features achieved an AUC of 0.86, comparing favorably to the size and shape model (AUC = 0.82). These findings validate CRM as a meaningful morphological feature that, when analyzed through radiomics, captures subtle yet important surface characteristics that distinguish rupture status.

Figure 2. Examples of CRM processing for ruptured and unruptured aneurysms. A, Example of the processing pipeline for ruptured aneurysms. Detailed mapping from 3D CRM to a 2D image. **B,** Example of the processing pipeline for unruptured aneurysms. Detailed mapping from 3D CRM to a 2D image. Note the increased surface heterogeneity and high-intensity protrusions in ruptured aneurysms. 2D indicates 2-dimensional; 3D, 3-dimensional; ACOM, anterior communicating artery; CRM, centroid radii model; ICA, internal carotid artery; MCA, middle cerebral artery; and PCOM, posterior communicating artery.

Downloaded from http://ahajournals.org by on April 6, 2026

The innovative use of radiomics in the evaluation of surface-derived features such as CRM opens exciting opportunities for future research, offering a fresh perspective on the understanding of aneurysmal rupture. Radiomics demonstrates a strong ability to discriminate the ruptured status of aneurysms based on CRM-derived imaging, providing valuable insights that might otherwise go unnoticed using traditional processing tools.

This approach can be readily extended to other surface scalar maps beyond CRM, such as curvature maps (including mean and Gaussian curvature), surface protrusion metrics (such as shape index and convexity index), and spherical deviation measures. These additional features could capture complementary aspects of aneurysm surface morphology, providing a richer and more detailed morphological characterization. Future studies would also combine surface-based radiomics features with hemodynamic parameters to create a robust and comprehensive risk assessment framework. Such integration could further enhance our understanding of rupture mechanisms and guide personalized aneurysm management strategies.

Although our current work remains a proof-of-concept study, its translation into clinical practice could, in the future, enable more refined risk stratification and support decisions regarding monitoring and potential intervention. Implementation into clinical workflows would require further technical development, including automation of high-quality surface segmentation, integration into image analysis pipelines, and validation across multicenter data sets.

Study Limitations

This study is retrospective and relies on the assumption that the aneurysm surface geometry captured at the time of imaging remains representative of the prerupture state. Although this assumption is commonly applied and supported by prior studies,[20] postrupture remodeling effects cannot be entirely excluded, and conclusive data are still needed. Furthermore, the statistical findings and predictive performance presented in this study require validation on independent data sets to confirm generalizability and robustness. Additional prospective and longitudinal studies are warranted to further validate both the clinical applicability of CRM radiomics in risk prediction and the stability of the statistical models and selected features across diverse populations and imaging cohorts.

CONCLUSION

We present a novel surface-based radiomics approach using the CRM to evaluate aneurysmal morphology. Our analysis of CRM-derived images showed that ruptured aneurysms are characterized by increased complexity and heterogeneity, reflecting irregular spatial characteristics. Multivariate analysis for rupture status discrimination achieved an AUC value of 0.86 (specificity 0.81, sensitivity 0.78). Radiomics texture analysis of CRM-mapped images demonstrated strong discriminative power for rupture status, outperforming established size and shape parameters. This approach, which extends the current use of radiomics beyond traditional medical imaging data, represents a new application of radiomics to geometric surface models and may offer new insight into morphological risk factors associated with aneurysm rupture.

ARTICLE INFORMATION

Received May 2, 2025; Accepted August 12, 2025

Affiliation

Cerebrovascular Hemodynamics Laboratory, Department of Neurosurgery, Tufts Medical Center and Tufts University School of Medicine, Boston, MA

Acknowledgments

The authors have nothing to report.

Sources of Funding

None.

Disclosures

None.

Supplemental Materials

Supplement Table 1: Univariate statistical analysis of selected CRM Radiomics descriptors for rupture status discrimination. Shown are mean and standard deviation. Statistical significance was assumed for $p<0.05$. AUC represents the area under the ROC curve. Results reflect CRM data following scaling by 100. More details on Radiomics features descriptors available at https://pyradiomics.readthedocs.io/en/latest/features.html.

STROBE Statement: Checklist of items that should be included in reports of observational studies.

REFERENCES

1. Wiebers DO, Whisnant JP, Huston J, 3rd, Meissner I, Brown RD, Jr., Piepgras DG, Forbes GS, Thielen K, Nichols D, et al. Unruptured intracranial aneurysms: natural history, clinical outcome, and risks of surgical and endovascular treatment. *Lancet*. 2003;362:103-110.
2. Ma BS, Harbaugh RE, Raghavan ML. Three-dimensional geometrical characterization of cerebral aneurysms. *Ann Biomed Eng*. 2004;32:264-273.
3. Raghavan ML, Ma B, Harbaugh RE. Quantified aneurysm shape and rupture risk. *J Neurosurg*. 2005;102:355-362.
4. Millán RD, Dempere-Marco L, Pozo JM, Cebral JR, Frangi AF. Morphological characterization of intracranial aneurysms using 3-D moment invariants. *IEEE Trans Med Imaging*. 2007;26:1270-1282. https://doi.org/10.1109/tmi.2007.901008
5. Rohde S, Lahmann K, Beck J, Nafe R, Yan B, Raabe A, Berkefeld J. Fourier analysis of intracranial aneurysms: towards an objective and quantitative evaluation of the shape of aneurysms. *Neuroradio*. 2005;47:121-126.
6. Lauric A, Miller EL, Baharoglu MI, Malek AM. 3D shape analysis of intracranial aneurysms using the writhe number as a discriminant for rupture. *Ann Biomed Eng*. 2011;39:1457-1469. https://doi.org/10.1007/s10439-010-0241-x

Downloaded from http://ahajournals.org by on April 6, 2026

7. Lauric A, Miller EL, Baharoglu MI, Malek AM. Rupture status discrimination in intracranial aneurysms using the centroid-radii model. *IEEE Trans Biomed Eng*. 2011;58:2895-2903.
8. van Griethuysen JJM, Fedorov A, Parmar C, Hosny A, Aucoin N, Narayan V, Beets-Tan RGH, Fillion-Robin JC, Pieper S, Aerts H. Computational radiomics system to decode the radiographic phenotype. *Cancer Res*. 2017;77:e104-e107. 10.1158/0008-5472.Can-17-0339
9. Zhang Y, Ma C, Liang S, Yan P, Liang F, Guo F, Jiang C. Morphologic feature elongation can predict occlusion status following pipeline embolization of intracranial aneurysms. *World Neurosurg*. 2018;119:e934-e940. https://doi.org/10.1016/j.wneu.2018.08.007
10. Ludwig CG, Lauric A, Malek JA, Mulligan R, Malek AM. Performance of Radiomics derived morphological features for prediction of aneurysm rupture status. *J Neurointerv Surg*. 2021;13:755-761. https://doi.org/10.1136/neurintsurg-2020-016808
11. Liu Q, Jiang P, Jiang Y, Ge H, Li S, Jin H, Li Y. Prediction of aneurysm stability using a machine learning model based on pyradiomics-derived morphological features. *Stroke*. 2019;50:2314-2321. https://doi.org/10.1161/strokeaha.119.025777
12. Lauric A, Ludwig CG, Malek AM. Enhanced radiomics for prediction of rupture status in cerebral aneurysms. *World Neurosurg*. 2022;159:e8-e22.
13. Chen G, Lu M, Shi Z, Xia S, Ren Y, Liu Z, Liu X, Li Z, Mao L, Li XL, et al. Development and validation of machine learning prediction model based on computed tomography angiography–derived hemodynamics for rupture status of intracranial aneurysms: a Chinese multicenter study. *Eur Radiol*. 2020;30:5170-5182. https://doi.org/10.1007/s00330-020-06886-7
14. Yamanouchi M, Arimura H, Kodama T, Urakami A. Prediction of intracranial aneurysm rupture risk using non-invasive radiomics analysis based on follow-up magnetic resonance angiography images: a preliminary study. *Appl Sci*. 2022;12:8615.
15. Podgorsak AR, Rava RA, Shiraz Bhurwani MM, Chandra AR, Davies JM, Siddiqui AH, Ionita CN. Automatic radiomic feature extraction using deep learning for angiographic parametric imaging of intracranial aneurysms. *J Neurointerv Surg*. 2020;12:417-421. https://doi.org/10.1136/neurintsurg-2019-015214
16. Shiraz Bhurwani MM, Waqas M, Podgorsak AR, Williams KA, Davies JM, Snyder K, Levy E, Siddiqui A, Ionita CN. Feasibility study for use of angiographic parametric imaging and deep neural networks for intracranial aneurysm occlusion prediction. *J Neurointerv Surg*. 2020;12:714-719. https://doi.org/10.1136/neurintsurg-2019-015544
17. Baharoglu MI, Lauric A, Gao B-L, Malek AM. Identification of a dichotomy in morphological predictors of rupture status between sidewall- and bifurcation-type intracranial aneurysms. *J Neurosurg*. 2012;116:871-881. https://doi.org/10.3171/2011.11.JNS11311
18. Mullen T. *Mastering blender*. John Wiley & Sons; 2011.
19. Peduzzi P, Concato J, Kemper E, Holford TR, Feinstein AR. A simulation study of the number of events per variable in logistic regression analysis. *J Clin Epidemiol*. 1996;49:1373-1379. https://doi.org/10.1016/S0895-4356(96)00236-3
20. Asari S, Ohmoto T. Natural history and risk factors of unruptured cerebral aneurysms. *Clin Neurol Neurosurg*. 1993;95:205-214.

Downloaded from http://ahajournals.org by on April 6, 2026